

Characterizing the controls on surface alkalinity in Nootka Sound, British Columbia

Senior Thesis Manuscript

June 2015

Una Miller

University of Washington

School of Oceanography

1501 NE Boat Street

Seattle, WA 98195

unam@u.washington.edu

Acknowledgments

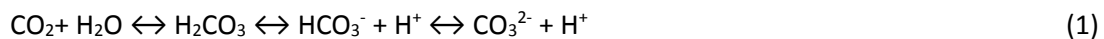
I would first like to thank the instructors of our senior thesis class, particularly Julian Sachs, my advisor, whose patience, knowledge, and enthusiasm brought me from an idea to a finished project, Arthur Nowell, whose cheerful help and encouragement were greatly appreciated and often needed, and Kathy Newell, who graciously helped us acquire everything from pipette tips to hundreds of sampling bottles. Also thank you to Jim Murray and Alex Gagnon for answering myriads of questions on the concept of alkalinity, to Evan Solomon and his graduate students for making it possible for me to run IC analysis, and to Ginger Armbrust's lab for allowing us to use their DIC analytical system. Many thanks to Claire Knox for her support throughout the development of our projects, to David Thoreson and the rest of the *R/V Weelander* group, especially Matthew Morris, for help out in the field, and to the crew of the *R/V Thompson*. Lastly, thank you to my fellow seniors, many of whom I have known since sophomore year and have enjoyed befriending since.

Abstract

Understanding the processes that alter alkalinity in estuarine systems is essential to understanding distributions of surface ocean alkalinity and by extension, atmospheric CO₂ levels, as a whole. Biological activity and mixing of distinct riverine sources can alter alkalinity before it reaches the open ocean, where it plays a significant role in the capacity of water to buffer against pH change, an important concept especially in the context of climate change. This study characterizes surface water alkalinity in the month of December in Nootka Sound, one of several large fjord systems on the west coast of Vancouver Island, British Columbia. Measurements of alkalinity, dissolved inorganic carbon (DIC), salinity, and nutrients are used to constrain the major processes controlling it. Results show that alkalinity is largely conservative in both of the inlets studied, with no significant biological controls.

1. Introduction

The role of alkalinity in the uptake of atmospheric CO₂ by the world's oceans has made characterizing its surface distribution increasingly important in the context of anthropogenic climate change. The ocean is thought to absorb 30-40% of CO₂ emissions from the burning of fossil fuels (Feely et al., 2004; Millero, 2007), a process that while mitigating increases in atmospheric CO₂, also results in what is known as ocean acidification. CO₂ reacts with water according to the following equation:



The dissociation of carbonic acid (H₂CO₃) into bicarbonate (HCO₃⁻) and hydrogen ions (H⁺) creates more acidic conditions that correspond with a lower pH. The more atmospheric concentrations of CO₂ increase, the more CO₂ is dissolved into the ocean, and the more pH is lowered. Surface ocean pH has decreased by 0.1 since the start of the industrial revolution (IPCC, 2014), and with unabated CO₂ emissions, could further decrease in the coming centuries by as much as 0.7, a pH change greater than any seen in the past 300 Myr (Caldiera and Wickett, 2003). These changes in pH would be much greater,

however, if not for the uptake of hydrogen ions by carbonate ions (CO_3^{2-}) to form bicarbonate (eq. 1). This reaction buffers changes in pH but also makes carbonate less available to calcifying organisms such as corals and calcareous plankton. The impacts of ocean acidification both on individual species and on ecosystems are only beginning to be understood (Feely et al., 2004, 2010; Orr, 2005; Millero, 2007).

The carbonate system is a set of equations and parameters that describe the system of CO_2 and other inorganic carbon species in water (eq. 1). The carbonate system parameters consist of $p\text{CO}_2$, $[\text{CO}_2]$, $[\text{HCO}_3^-]$, $[\text{CO}_3^{2-}]$, pH, dissolved inorganic carbon (DIC), and alkalinity, of which only $p\text{CO}_2$, pH, DIC, and alkalinity can be measured directly. However, if two of the parameters are known, the rest can be calculated. Models such as those described by Lauvset et al. (2015) and Tjiputra (2014) calculate large-scale distributions of surface ocean pH and $p\text{CO}_2$ in this way. Alkalinity in particular is often used in these calculations because of the accuracy associated with its analytical technique as well as its largely conservative nature in mixing, which makes it ideal for use in modeling (Dickson and Riley, 1978; Millero, 2007). Despite its use in carbonate system calculations and its close tie to the capacity of surface water to uptake CO_2 (Feely et al., 2004), described below, alkalinity data remain overall sparse. Efforts to provide large-scale spatial and temporal alkalinity datasets has led to the development of algorithms to calculate alkalinity from global temperature and salinity datasets (Millero et al., 1998; Lee et al., 2006) and from nitrate (NO_3^-) concentrations (Evans et al., 2013), as well as moorings for autonomous *in-situ* alkalinity measurements (Spaulding et al., 2014).

Alkalinity can be thought of as the capacity of water to buffer against changes in pH, an interpretation that arises from a more formal definition as the charge imbalance of the conservative ions in water (Zeebe and Wolf-Gladrow, 2001), shown here with the major ions in seawater:

$$\begin{aligned} & [\text{Na}^+] + 2[\text{Mg}^{2+}] + 2[\text{Ca}^{2+}] + [\text{K}^+] - [\text{Cl}^-] - [2(\text{SO}_4^{2-})] - [\text{NO}_3^-] = \text{Alkalinity} \\ & = [\text{HCO}_3^-] + 2[\text{CO}_3^{2-}] + [\text{B}(\text{OH})_4^-] \end{aligned} \tag{2}$$

The imbalance of charge on the left side of the equation between conservative cations such as sodium (Na^+) and conservative anions such as chloride (Cl^-) is compensated for on the right side by the exchange of hydrogen ions between acids and bases in order to achieve an overall neutral charge in water. The greater the concentrations of ions on the right side, the greater the capacity of seawater to exchange hydrogen ions to counteract changes in pH, such as from CO_2 incursion (eq. 1). The most comprehensive definition of alkalinity is given by Wolf-Gladrow et al. (2007), which accounts for various biogeochemical processes not considered in the earlier definition of “exact” total alkalinity (TA) given by Dickson (1981) .

Processes that change the concentrations of ions on either side of the equation will change alkalinity. Ocean alkalinity is sourced from rivers, primarily in the form of bicarbonate weathered from carbonate rocks, and is therefore largely a function of salinity. A strong linear relationship between alkalinity and salinity typically exists in the open surface ocean, but can break down in coastal and estuarine systems, where mixing of distinct freshwater sources, lateral alongshore currents, upwelling, and biological activity can cause deviations (Cai et al., 2010). Because river alkalinity is greatly altered by estuarine and coastal processes before ultimately reaching the open ocean, understanding the influences and distributions of alkalinity in these systems is important to our understanding of ocean alkalinity as a whole (Hoppema, 1990; Hydes and Hartman, 2011).

Nootka Sound is one of several large estuarine fjord systems on the west coast of Vancouver Island, British Columbia. While Tully (1937) and Pickard (1963) provide a general oceanographic characterization of the sound, unlike nearby estuaries such as Saanich Inlet and the Puget Sound, Nootka Sound remains largely unstudied. This study characterizes the distribution of and influences on surface alkalinity in Nootka Sound during the month of December.

Aside from mixing of freshwater and seawater endmembers, there are several biogeochemical processes that could exert significant influence on surface alkalinity in Nootka Sound, the principal of

which is the formation and dissolution of calcium carbonate (CaCO_3) (Friis, 2003). Calcium carbonate is produced biogenically in the water column by coccolithophorids, foraminifera, pteropods, and corals according to



in which the precipitation of 1 mole of calcium carbonate results in a decrease in alkalinity by 2 moles, represented in this case by bicarbonate ions. Likewise, calcium carbonate dissolution increases alkalinity by 2 moles.

The photosynthetic uptake of nutrients, nitrogen compounds in particular, is also known to affect alkalinity (Wolf-Gladrow et al., 2007). Brewer and Goldman (1976) and Goldman and Brewer (1980) examined the uptake of nitrogen species by photosynthetic organisms and found an empirical 1:1 stoichiometric increase in alkalinity with nitrate (NO_3^-) and nitrite (NO_2^-) uptake and a 1:1 decrease with ammonia uptake. Kim and Lee (2009) reexamined the stoichiometric relationship between nitrate and alkalinity and found it to be less than 1:1 when the release of dissolved organic matter (DOM) by phytoplankton was also taken into account. In addition, Kim et al. (2006) described the influence of particulate organic matter (POM) on alkalinity as non-negligible. For the purposes of this study, however, only nitrate, the major nitrogen compound in marine environments, will be considered and a 1:1 stoichiometry will be assumed.

Biological processes that occur in anoxic bottom water and sediments also affect alkalinity (Berner and Scott, 2003; Knull and Richards, 1969; Hiscock and Millero, 2006). The process considered in this study is the oxidation of methane (CH_4) by sulphate reduction, whereby the production of bicarbonate and hydrogen sulfide (HS^-) increases alkalinity by two moles for every one mole of sulphate reduced (Wolf-Gladrow et al. 2007):



The presence of anoxic conditions is common in fjords such as the inlets of Nootka Sound, where the circulation of bottom water is limited. If anoxic bottom water containing the products of sulphate reduction were mixed to the surface, alkalinity would be increased.

These hypothesized controls on alkalinity in Nootka Sound are summarized in Figure 1 and the examination of their relative significance during the month of December will be the focus of the remainder of this paper.

2. Methods

2.1 Alkalinity and DIC water sample collection and analysis

Surface water samples for alkalinity and DIC analysis were collected in December 2014 from the small work boat *R/V Weelander*. A total of 36 water samples were collected across two of the three inlets: 21 in Muchalat Inlet, and 15 in Tahsis Inlet (Fig. 2). Sites were spaced evenly and along the entire length of each inlet. At each site, 500 mL of water were collected in borosilicate bottles held at the surface with the opening half submerged as to allow displaced air to escape. A small volume of water was then poured out to allow for thermal expansion. Samples were poisoned with 100 µg of saturated mercuric chloride (HgCl₂) for every 250 mL of water collected and sealed with an Apiezon greased stopper and a rubber band. Salinity was measured at each of these sites with a YSI Data Sonde.

Freshwater samples were collected from Gold River, Tahsis River, and various other rivers, creeks, streams, and waterfalls, totaling to five in Muchalat and eight in Tahsis. When shallow water depth prohibited sampling the freshwater source directly, water was collected where salinity was lowest in the nearby area. Sample collection and preparation methodology are as described above.

Conductivity, temperature, and depth (CTD) casts were deployed from the *R/V Thompson* in both inlets as well as in the open ocean approximately 70 km seaward from the mouth of Nootka Sound. Casts were deployed in the inlets where depth was greatest and therefore where the presence of anoxic

bottom water would be most likely. Water samples were collected from each cast at depths representative of the water column, e.g. at minimum, one each at the deepest and shallowest depths and one in the mixed layer. The samples were prepared according to the Pacific Marine Environmental Laboratory (PMEL) sampling protocol.

Alkalinity titrations were performed with the Radiometer Co. PHM85 Precision pH meter and ABU 80 Auto-Burette. Alkalinity values were converted from the reported units of g CaCO₃ L⁻¹ to μmol CaCO₃ kg⁻¹ with densities calculated according to the algorithm given in the 44th issue of Technical Papers in Marine Science (UNESCO, 1983). For the remainder of this paper, alkalinity units will be given in μeq kg⁻¹, which are “equivalent” units of alkalinity equal to twice the value of μmol CaCO₃ kg⁻¹. Analysis precision was equal to or greater than 20 μeq kg⁻¹.

DIC measurements were made on the Apollo Scitech AS-C3 DIC analyzer with a precision of 15 μeq kg⁻¹.

2.2 Nutrient water sample collection and analysis

Following the detection of anoxic bottom water in Muchalat Inlet, water samples were collected from the CTD cast for a suite of nutrient concentration analyses, which included nitrate, nitrite, silicate, ammonia, sulphate, and phosphate. Additional water samples for sulphate were collected in the surface water at seven of the aforementioned surface sampling sites in Muchalat Inlet. Water samples for sulphate analysis were treated with zinc acetate in a ratio of 0.1 mL zinc acetate for every 1 mL of water. All samples for nutrient analysis were stored at subzero temperature to prohibit biological activity.

Concentrations of sulphate were measured via ion chromatography on a Metrohm 882 Compact IC plus. The remaining nutrient concentrations were measured via continuous flow analysis with the Technicon AAll System.

3. Results

3.1 Variation with salinity

Figure 3a shows alkalinity distribution across Muchalat and Tahsis Inlets. Surface water alkalinity in Muchalat Inlet ranged from 211 to 624 $\mu\text{eq kg}^{-1}$ and averaged to 404 $\mu\text{eq kg}^{-1}$. Tahsis Inlet values were overall much higher, ranging from 81.5 to 1140 $\mu\text{eq kg}^{-1}$ and averaging to 738 $\mu\text{eq kg}^{-1}$. This contrast is mirrored in surface salinities (Fig. 3b), which ranged from 0.71 to 7.96 in Muchalat Inlet and 7.8 to 21.12 in Tahsis Inlet. The surface alkalinity-salinity relationship is strongly linear in Muchalat (Fig. 4) but much less so in Tahsis, where alkalinity values plateau between salinities of 10-20 PSU (Fig. 5). Linear regression of all surface alkalinity values and all freshwater alkalinity values against salinity yielded r^2 values of 0.93 and 0.81 in Muchalat and Tahsis, respectively. Excluding freshwater values in Muchalat did not affect the r^2 value while including only Gold River increased it to 0.94. In Tahsis, excluding all freshwater values drastically lowered the r^2 value to 0.26 and including only Tahsis River lowered it to 0.68. These linear regression models of alkalinity and salinity extrapolated to high salinities fall shy of the seawater mixing endmember values in both of the inlets (Fig 4 and 5). Water column alkalinity also exhibits a linear relationship with salinity and again, this relationship is stronger in Muchalat (Fig 6).

3.2 Variation with DIC

There is an approximately 1:1 relationship between both surface alkalinity and DIC and water column alkalinity and DIC in Muchalat and Tahsis (Fig.7). Within the anoxic bottom water of Muchalat, there is an increase in alkalinity of 58 $\mu\text{eq kg}^{-1}$ and an increase in DIC of 24 $\mu\text{mol kg}^{-1}$, a roughly 2:1 change.

3.3 Variation with depth

Both alkalinity and DIC show a general increase with depth in both inlets (Fig 8 and 9). In Muchalat, alkalinity increases by 1900 $\mu\text{eq kg}^{-1}$ from the surface to the first measurement at depth, 40

m. In Tahsis, a similarly drastic increase of $1130 \mu\text{eq kg}^{-1}$ occurs in the first 40m of depth. Near constant temperature and salinity profiles below the mixed layers in both inlets show little to no vertical mixing.

A strong hydrogen sulfide odor was detected in the bottom water sample in Muchalat Inlet, indicating the occurrence of sulphate reduction. This is supported by oxygen and nitrate concentrations at depth, which reach zero in sequence (Fig 8). Sulphate concentrations do not show a decrease, but this does not preclude sulphate reduction as the olfactory detection of hydrogen sulfide is a much more sensitive, if not less quantitative, test than sulphate ion chromatography. Alkalinity shows an increase of approximately $60 \mu\text{eq kg}^{-1}$ from 300 m to 350 m of depth, the depth interval in which anoxic conditions are present. This would correspond with a $30 \mu\text{eq kg}^{-1}$ decrease in sulphate if all of this change were due to sulphate reduction. Sulphate was measured in units of mmol kg^{-1} , three orders of magnitude greater than this theoretical maximum change in concentration, and it is therefore likely that the method of analysis was not sensitive enough to quantify this change in sulphate within the anoxic layer. No hydrogen sulfide was detected in the bottom water of Tahsis, and the oxygen profile does not indicate the presence of anoxic bottom water (Fig 9).

4. Discussion

4.1 Muchalat Inlet

That the alkalinity-salinity data in Muchalat fits a linear regression so well indicates that mixing is the primary influence on alkalinity in this inlet. Corroborating this is the 1:1 relationship between DIC and alkalinity in both surface and water column measurements, which indicates that the processes dictating alkalinity are equally affecting DIC. DIC is defined as the sum of the concentrations of carbon dioxide, bicarbonate, and carbonate. Calcification (eq. 3), which decreases alkalinity by two moles, also produces one mole of carbon dioxide and therefore its effect on alkalinity and DIC is 2:1. Likewise, sulphate reduction (eq. 4) increases alkalinity by two moles while increasing DIC by one with the production of one mole of bicarbonate. The overall 1:1 relationship between alkalinity and DIC in

Muchalat precludes calcification and dissolution as significant processes in both surface waters and in the water column, and while an approximately 2:1 relationship is observed within the anoxic bottom water, temperature and salinity profiles show no mixing of this sulfidic deep water to the surface. It also precludes photosynthetic nitrate uptake, which along with the associated CO₂ uptake affects alkalinity and DIC in a ratio much smaller than 1:1. A calculation of the maximum stoichiometric change in alkalinity from nitrate uptake upholds the insignificance of this process. Nitrate concentrations at a depth of 30 m ranged from 10-12 µM over the length of the inlet, and assigning these values as the maximum surface concentrations and assuming all of it to be taken up by phytoplankton yields a maximum 10-12 µeq kg⁻¹ change in alkalinity. Not only is this range below the analytical precision of 20 µeq kg⁻¹ and therefore insignificant, this calculation assumes mixing of water at depth with the surface in what is a system with a highly stratified surface layer; the actual surface concentrations of nitrate are almost certainly much lower. Nitrate uptake and calcification can be concluded to exert no significance influence on surface alkalinity in Muchalat Inlet, which agrees with the generally low productivity experienced during winter months and the relative scarcity of calcifying phytoplankton in surface waters of this region (Jim Murray, personal communication). Products of sulphate reduction increase alkalinity at depth but do not appear to be upwelled, leaving surface alkalinity unaffected.

The linear regression of the data suggests not only that mixing is dominant but that mixing is between a single seawater and a single freshwater endmember value. This freshwater endmember is Gold River, the dominating influence of which can be seen in the overall low salinity of Muchalat Inlet. Accordingly, including only Gold River in the linear regression resulted in the highest r² value. Therefore, surface alkalinity in Muchalat can be modeled with the equation given by this regression:

$$\text{Alkalinity} = 52.453 * \text{Salinity} + 163.07 \quad (5)$$

The seawater (S=34) endmember as extrapolated from this equation is 1950 µeq kg⁻¹, which falls short of the 2120 µeq kg⁻¹ measured in the open ocean surface. Another possible endmember is the

water column within the inlet itself, which mixes with the surface when cold winter temperatures deepen the mixed layer. Conversely, greater precipitation in the winter can greatly limit this mixing through the formation of a freshwater lens. The latter appears to be the case as $1950 \mu\text{eq kg}^{-1}$ also falls short of water column alkalinity, which ranges from $2150 \mu\text{eq kg}^{-1}$ to $2300 \mu\text{eq kg}^{-1}$. The likely explanation is that the seawater endmember in this system is neither entirely ocean water nor bottom water, but water from just outside the inlet in the main sound, which is a mixture of ocean water and the water from other inlets. Unfortunately, no alkalinity data was collected to confirm this. However, the linear regression extrapolated to $S=20$ gives a value very close to those measured at the same salinity in Tahsis inlet, suggesting a shared mixing endmember sourced from the sound.

One deviation from what would be an otherwise straightforward mixing relationship between Gold River and an undetermined high salinity endmember outside of the inlet is the interruption of low alkalinity and seawater values throughout the inlet by a section of high salinity and alkalinity in the middle (Fig. 3). If Gold River were the only significant freshwater input, salinity and alkalinity values would increase steadily from the mouth of the river to the end of the inlet. This anomaly can be explained by the presence of rivers on either side of the inlet upstream of this anomaly (Fig. 2), which were unable to be sampled. Because biological activity alone would not produce the high alkalinity values in this area or explain the salinity anomaly, mixing of water from one or both rivers is the likely source of both the high salinity and alkalinity values. It is not uncommon for rivers in this area to be saline, as high tides can result in saltwater incursion upstream (David Thoreson, personal communication). In the neighboring Tlupana Inlet, salinity measured roughly 30 m upstream a large river was 12.69. Measurements in this area of Muchalat were taken in the early afternoon, with the lowest tide that day occurring at half past noon. It is feasible that at the time of sampling, water that had been pushed upstream in one or both of these rivers at high tide was emptying back into the inlet. The water coming from these rivers, whether sourced from further upstream or from the inlet, has the same

freshwater endmember as Gold River because the linear two endmember mixing relationship of salinity and alkalinity within this inlet is preserved.

4.2 Tahsis Inlet

Tahsis is immediately identifiable as a more complex system. Linear regression of the data gives a poorer linear fit and freshwater alkalinity values exhibit a much greater range. However, as in Muchalat, biological processes are of negligible significance. No anoxic bottom water and accompanying sulphate reduction were detected, and the 1:1 relationship of alkalinity and DIC observed in Tahsis rules out calcification and nitrate uptake. Additionally, measured surface nitrate concentrations ranged from 3-10 $\mu\text{mol kg}^{-1}$ around the mouth of Tahsis River and by the same logic as before, the maximum change in alkalinity caused by nitrate is less than the analytical precision of 20 $\mu\text{eq kg}^{-1}$ and therefore insignificant. This leaves the mixing of water bodies as the primary influence of alkalinity in Tahsis Inlet.

That the linear regression of all surface and freshwater data in Tahsis yielded an r^2 lower than in Muchalat, and that the inclusion of only Tahsis River lowered it further, is an indication of the presence of a freshwater endmember not captured by measurements made as part of this study. This points to water inflow from Tsowwin Narrows, which connects Tahsis Inlet with Esperanza Inlet to the West and represents a potential inflow of water much greater than from any of the rivers that feed into Tahsis inlet (Fig 2). No data were collected from Esperanza Inlet and therefore its freshwater endmember alkalinity values cannot be used to support this hypothesis directly, however Figure 3a shows a block of low salinity and alkalinity values downstream of Tsowwin Narrows, which would suggest that surface water in Tahsis Inlet is strongly influenced by input from Esperanza Inlet. In addition, the extremely poor fit of the surface measurements independent of any freshwater values suggests that unlike Muchalat, Tahsis is not a single endmember system but instead involves mixing of multiple freshwater sources, which in this case appear to be the rivers that feed both into Esperanza Inlet and Tahsis Inlet.

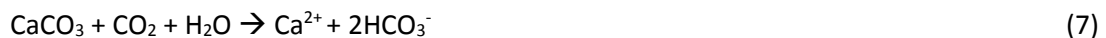
With the available data, surface alkalinity in Tahsis Inlet is best modeled by the equation produced from the linear regression of all surface and freshwater data, however the unaccounted freshwater endmembers and subsequent poor r^2 value must be taken into consideration.

$$\text{Alkalinity} = 44.282 * \text{Salinity} + 289.98 \quad (6)$$

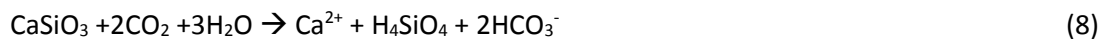
As in Muchalat, the model extrapolated to high salinity ($S=34$) gives an alkalinity value much lower than any open ocean or water column measurements and leaves the main sound as the most likely mixing endmember. It is conceivable that if additional surface measurements were made in Tlupana and Esperanza Inlets as well as in the main sound, the conservative mixing of alkalinity could be traced from its freshwater sources in each inlet, though the sound, and to the measured ocean endmember value.

4.3 River Alkalinity

The natural extension of a discussion regarding the alkalinity of a system dominated by the mixing of variable freshwater endmembers is the source of this variability. Freshwater alkalinity values ranged from 132 to 269 $\mu\text{eq kg}^{-1}$ in Muchalat and 81.5 to 455 $\mu\text{eq kg}^{-1}$ in Tahsis. The primary source of alkalinity is the weathering of carbonate and silicate rocks on land, the former of which is represented here by the weathering of calcium carbonate



and the latter of which can be represented as



according to Hieronymus and Walin (2013). In both cases, weathering of one mole of the mineral produces two moles of alkalinity. A bedrock map of Vancouver Island shows that the primary bedrock types surrounding Gold River, the dominant freshwater source of Muchalat Inlet, are granodioritic and feldspar porphyritic intrusive rocks (maroon color) and marine sedimentary volcanic rocks (peach color) (Fig. 10). The bedrock types surrounding Tahsis Inlet and the neighboring Esperanza Inlet include a large

stretch of marine sedimentary volcanic rock but are also primarily calc-alkaline volcanic rocks (plum color), limestone (salmon color), calcareous sedimentary rocks (dark salmon color), and limestone bioherms (lime green color). An accompanying surficial sediment map shows that land surrounding the areas of interest is mostly exposed bedrock or bedrock covered by ~1 m of sediment, making weathering of bedrock in the surrounding watershed an important control on the alkalinity that rivers transport into the inlets of Nootka Sound. That the bedrock surrounding Tahsis and Esperanza Inlets is both more varied and composed of more types of carbonate rock, which weathers more readily than silicates, than the bedrock surrounding Gold River could be directly related to the overall higher and more variable freshwater alkalinity values measured in Tahsis.

4.4 Comparison with other systems

The alkalinity measured in Muchalat and Tahsis agrees with regional findings in other studies. Lauerwald et al. (2013) reported riverine alkalinities of 200-1000 $\mu\text{eq kg}^{-1}$ in the Pacific Northwest area, which are relatively low compared with inland North America, where alkalinity reaches upwards of 4000 $\mu\text{eq kg}^{-1}$. Voss et al. (2014) reported values from nearby mainland rivers ranging from as low as 98 $\mu\text{eq kg}^{-1}$ to as high as 1936 $\mu\text{eq kg}^{-1}$. Alkalinity near Vancouver City in the Fraser River, the longest river in British Columbia, was reported to be 693 $\mu\text{eq kg}^{-1}$, about 200 $\mu\text{eq kg}^{-1}$ than the highest measured freshwater alkalinity in Tahsis Inlet.

Howland et al. (2000) characterized alkalinity trends in Tweed Estuary, UK monthly over a period of one year. They found alkalinity to be conservative in all months but July, during which measured dissolved oxygen saturations greater than 100% indicated significant photosynthetic activity in an otherwise year-round mixing dominated alkalinity scheme. Abril et al. (2003) and the references therein describe estuarine systems where dissolution of calcium carbonate and biological processes involving nitrogen species, such as nitrate uptake, were significant enough to deviate alkalinity from conservative behavior. In the case of the former, the estuaries were both highly productive and turbid, which

facilitated significant formation and dissolution of calcium carbonate. In the latter case, the estuaries were polluted or had large tidal marshes. The surface alkalinity in the inlets of the relatively pristine Nootka Sound resembles the simple mixing scheme described by Howland et al. (2000), at least during the week-long study period in the month of December. It is possible that biological processes play a much more significant role in alkalinity distributions during other parts of the year, especially in spring and summer when biological activity is greater.

4.5 Comparison with a global scale salinity-alkalinity model

Lee et al. (2006) derived a set of region specific algorithms that allow for the calculation of surface alkalinity from salinity and temperature in the open ocean. Alkalinity values calculated with the North Pacific algorithm using temperature and salinity data collected as part of this study are compared against their corresponding measured alkalinity values in figure 11. Although the model fails below salinities of 25, above this salinity it agrees with the measured values, all from CTD casts, within $100 \mu\text{eq kg}^{-1}$ in all but one instance. As expected, this global scale open ocean model cannot be applied to an estuarine system, however calculated values match well enough with the measured water column and ocean values that further comparison with measurements along the coast of Vancouver Island may show the algorithm to be accurate not only in the open ocean but in the dynamic coastal environment as well.

Conclusion

Estuaries are an important link between open ocean alkalinity and its riverine sources. Because the interactions of processes that control alkalinity vary across estuaries and over time within individual estuaries, studies of alkalinity such as this one, while small in scale, assist our understanding of larger scale alkalinity distributions. Surface alkalinity in the inlets of Nootka Sound during the winter is strictly conservative, with no significant biological controls. Although sulphate reduction was detected in the deep water of Muchalat Inlet, temperature and salinity profiles showed no mixing of this water to the

surface. Alkalinity in Muchalat was found to be overall much lower than in Tahsis, and can be modeled as a simple linear mixing relationship between Gold River and the main sound endmember. Alkalinity in Tahsis was found to be more complex, with no clear freshwater endmember. The influx of water from Esperanza Inlet via Tsowwin Narrows appears to exert a large influence on surface water in Tahsis and is a likely cause for this complexity, although no data was collected to directly confirm this. Weathering of differing types of bedrock in the drainage basins for each inlet are a plausible explanation for the differing ranges of freshwater alkalinity values, with the more calcareous and varied bedrock surrounding Tahsis correlating with higher and more varied freshwater alkalinity values. Although this study was able to characterize the controls on alkalinity in the month of December, the potential for seasonal variations in biological activity, river volume, turbidity, and mixing patterns, and the relative lack of alkalinity data in Vancouver Island as a whole, merits further study of surface alkalinity in Nootka Sound and surrounding areas.

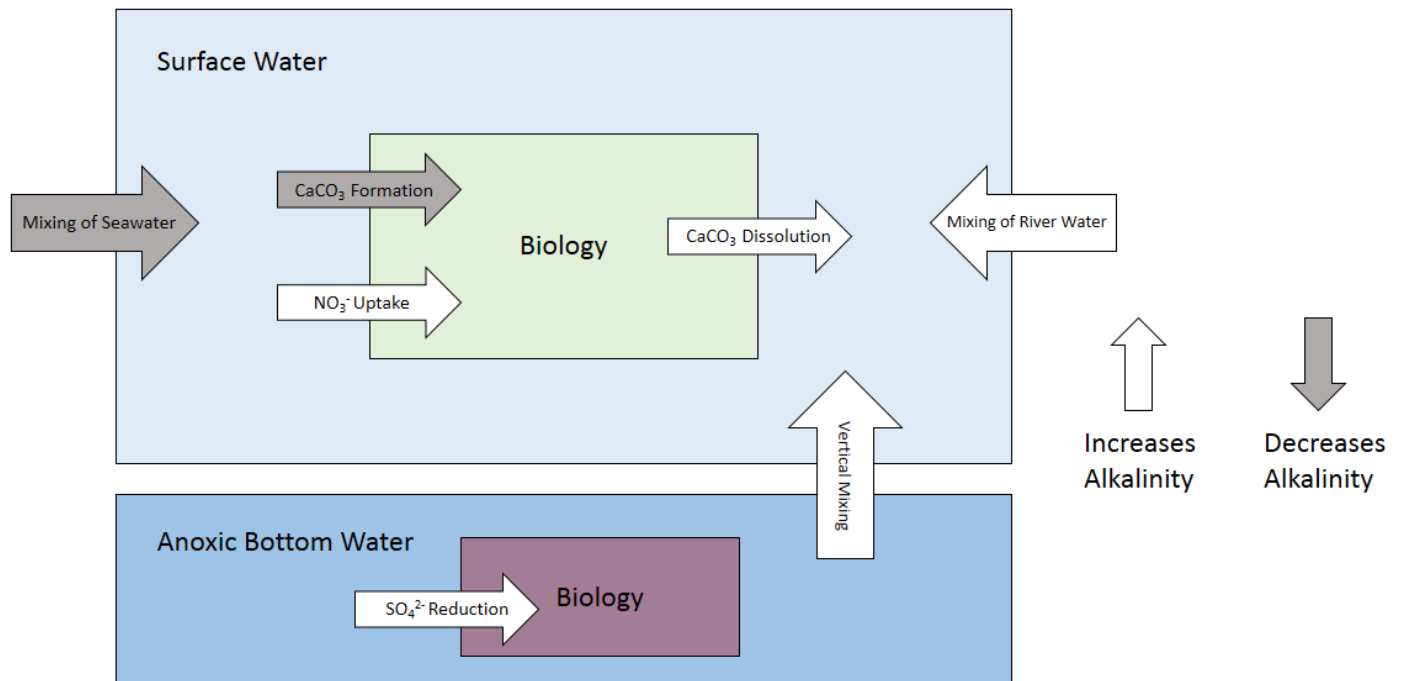


Fig. 1. A box model of major processes with the potential to affect alkalinity in the surface water of Nootka Sound.

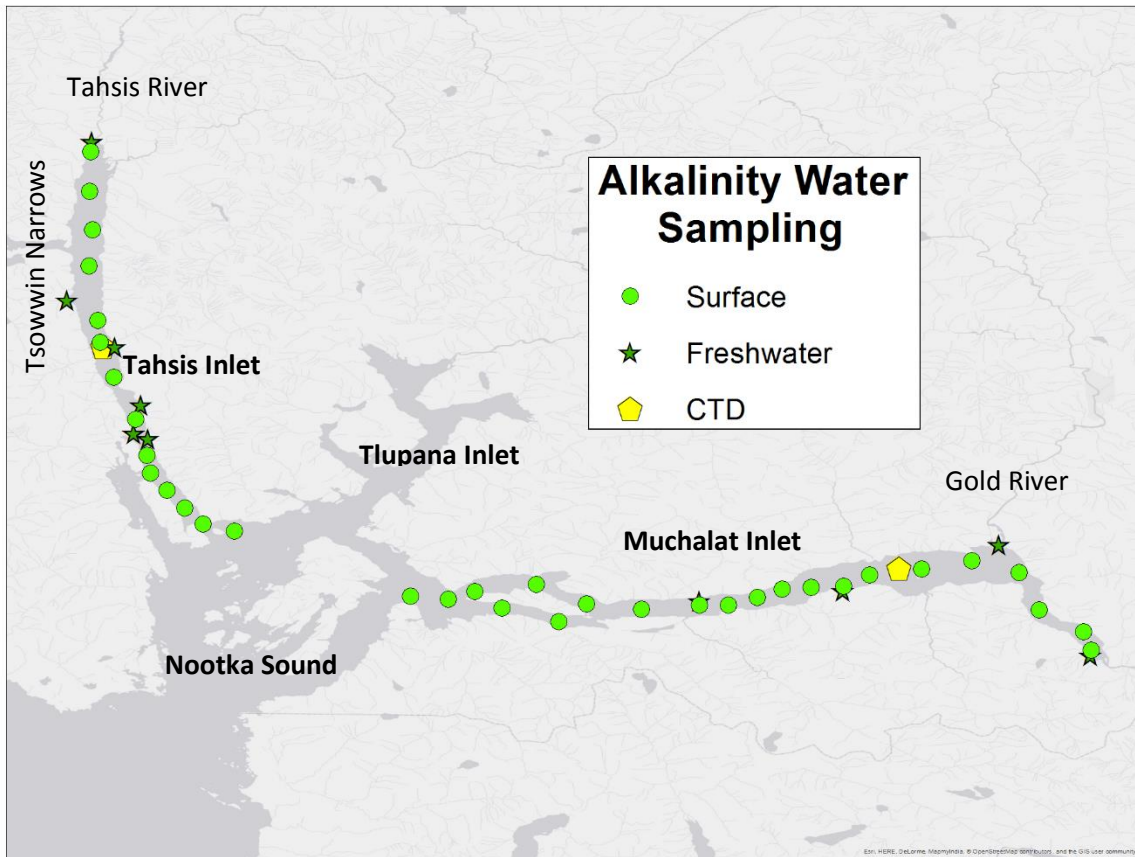


Fig. 2. Map of sampling stations. Not shown is the CTD cast deployed 70 miles seaward of the mouth of Nootka Sound.

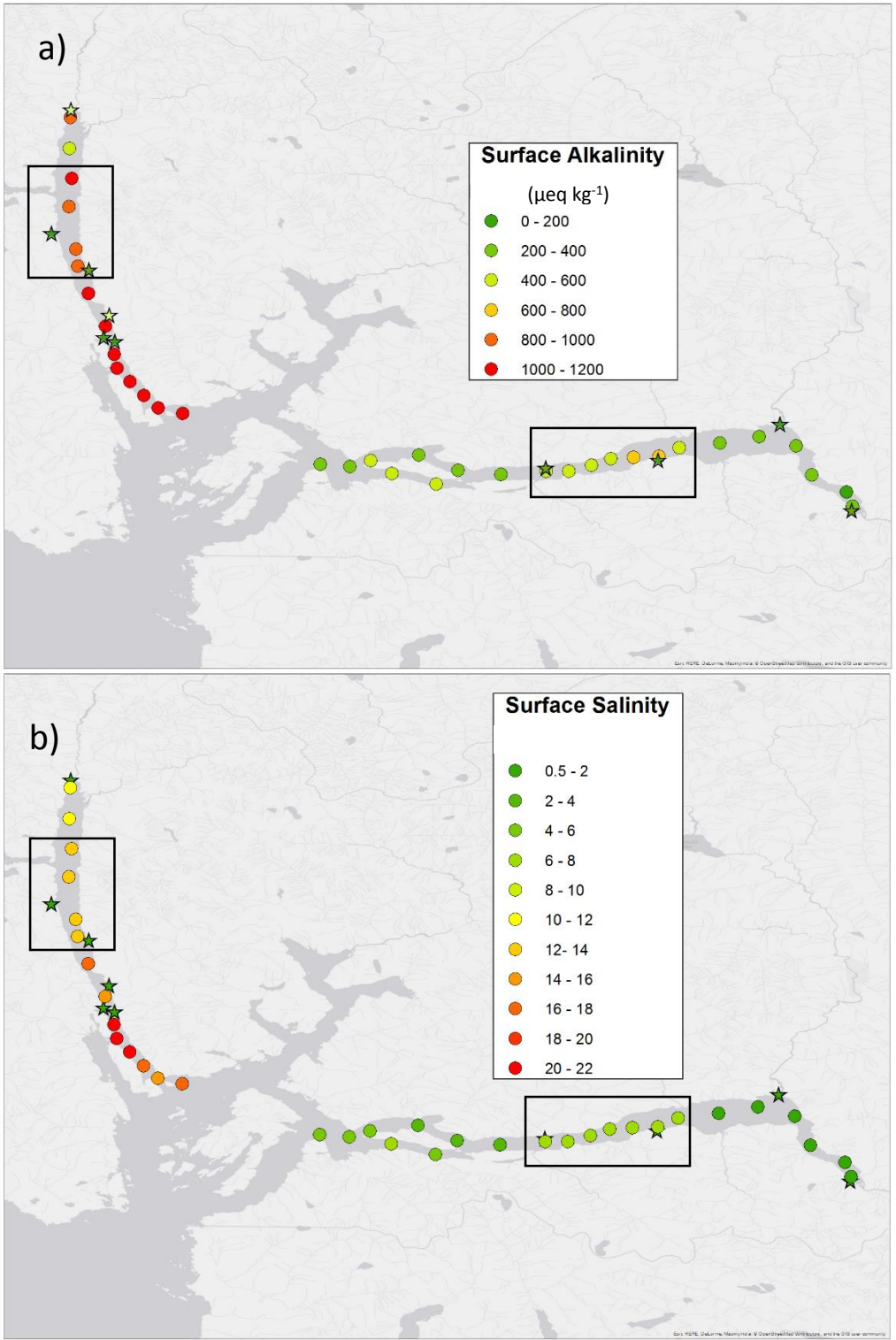


Fig. 3. Nootka sound showing a) alkalinity and b) salinity distributions across Muchlaet and Tahsis inlets. Stars indicate sites where freshwater samples were collected. Black boxes indicate the input of water from Tsowwin Narrows in Tahsis and from the hypothesized saline river(s) in Muchalat.

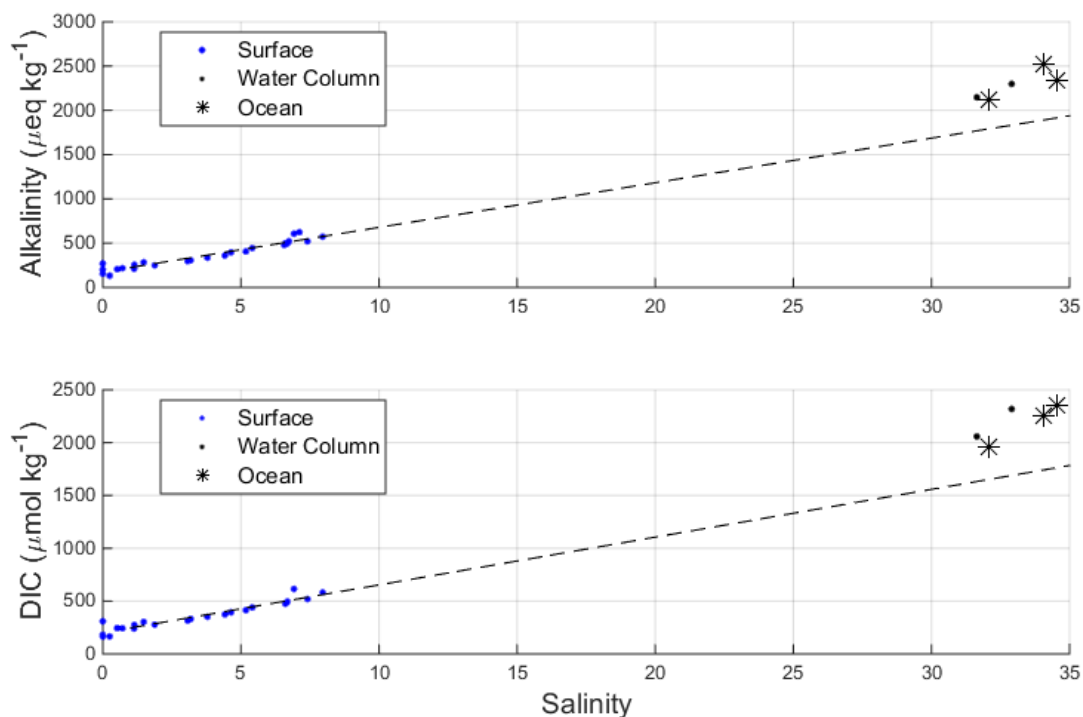


Fig. 4. Plots of surface salinity against alkalinity and DIC in Muchalat Inlet with water column and ocean mixing endmember values (in black). The linear fit given in equation 5 is shown. “Water Column” and “Ocean” values are from water samples collected with two CTD casts, one in Muchalat and the other in the open ocean. For clarity, only the shallowest and deepest measurements are included from the Muchalat CTD cast. In order of increasing salinity, the ocean measurements denoted by asterisks are from depths of 2, 500, 1700 meters.

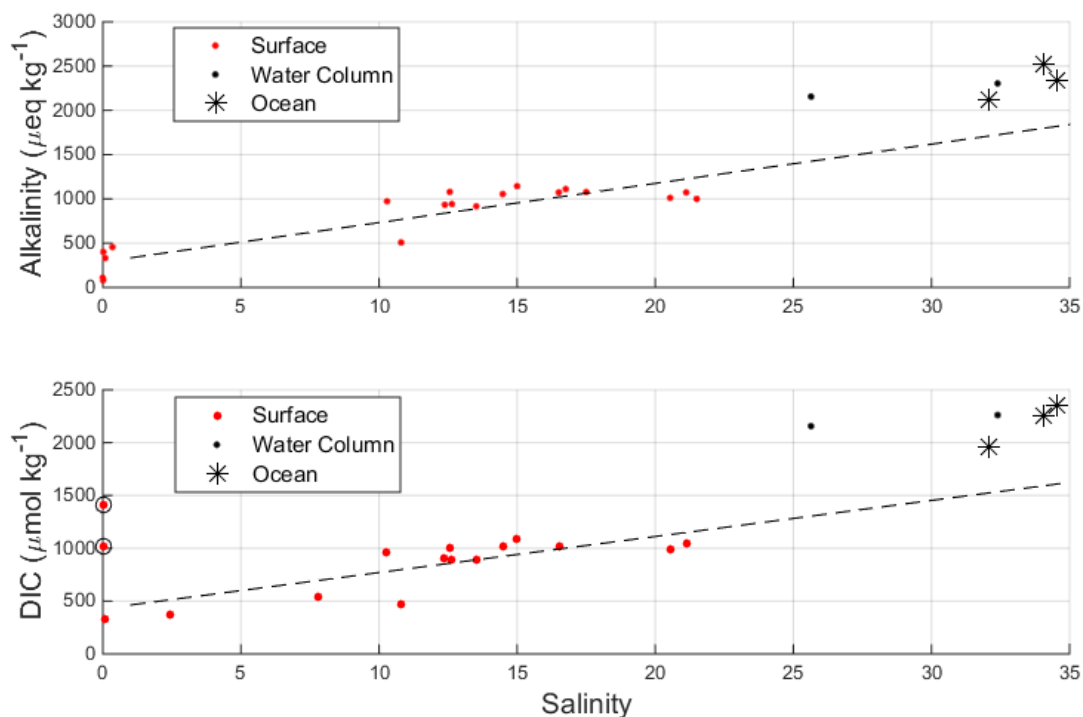


Fig. 5. Plots of salinity against alkalinity and DIC in Tahsis Inlet. The circled DIC values were likely the result of poor sampling technique and were excluded from line-fitting. The linear fit given in equation 6 is shown. “Water Column” and “Ocean” values are from water samples collected with two CTD casts, one in Tahsis and the other in the open ocean. For clarity, only the shallowest and deepest measurements are included from the Tahsis CTD cast. In order of increasing salinity, the ocean measurements denoted by asterisks are from depths of 2, 500, 1700 meters.

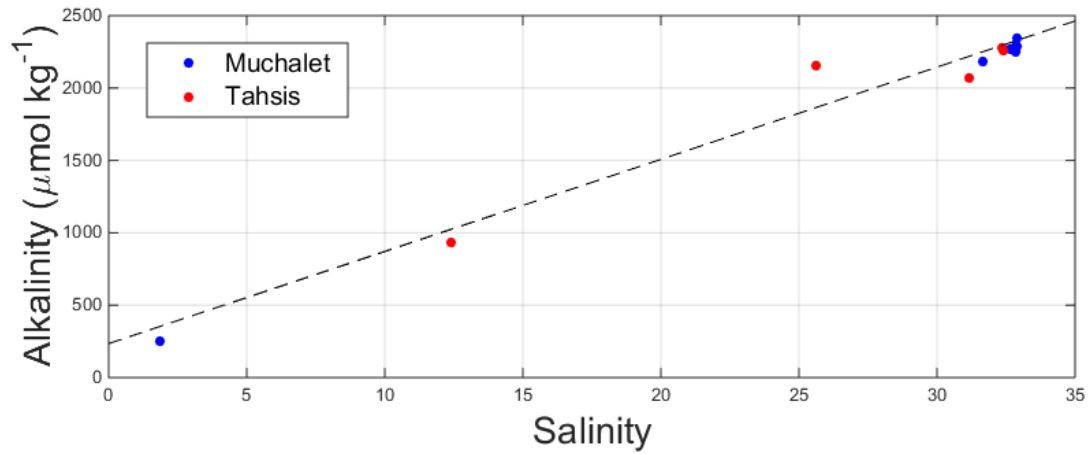


Fig. 6. Water column alkalinity values from water collected in CTD casts plotted against salinity. The lowest salinity values in each inlet are from the surface water samples collected closest to the cast location. Muchalat data fit the linear line $y=64.269x + 127.87$ with an r^2 value of 0.9986. Tahsis data fit the linear line $y=63.664x+234.49$ with an r^2 value of 0.9107. Only the latter line was included in the plot for clarity.

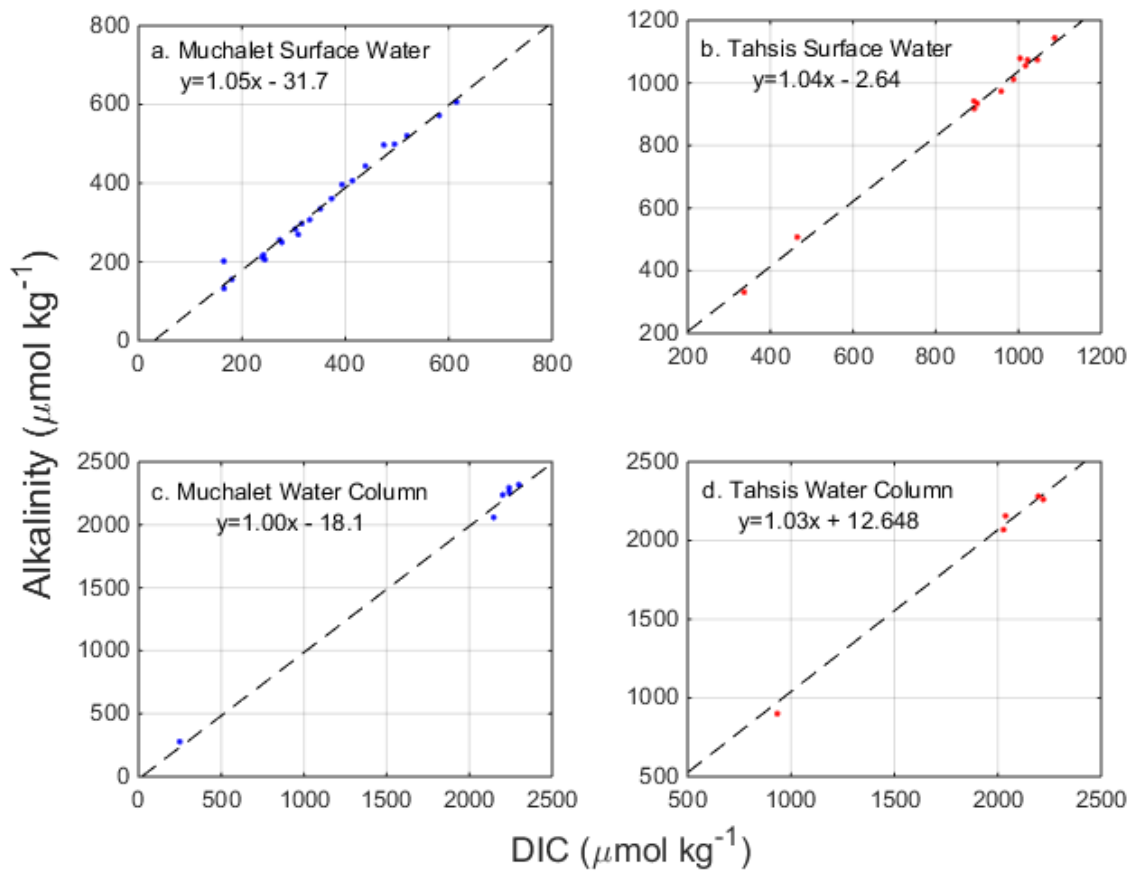


Fig. 7. Plots of surface and water column DIC against alkalinity in Muchalat and Tahsis, all showing a 1:1 relationship. The equations for the linear fit lines are provided in the upper left corner. The two anomalously high freshwater DIC values in Tahsis were excluded from the line fitting. Water column plots include one surface measurement taken at the surface station closest to the CTD cast location.

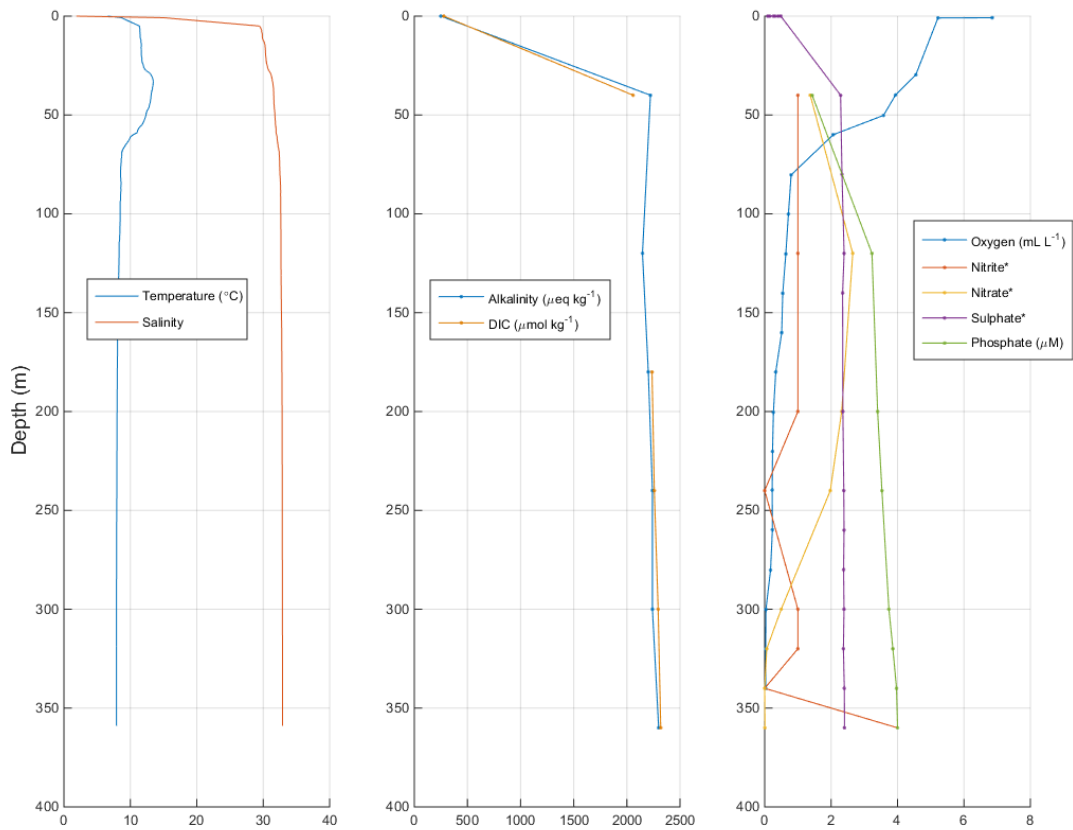


Fig. 8. Temperature, salinity, alkalinity, DIC, oxygen, and nutrient data from the CTD cast in Muchalat Inlet. Surface (depth of zero) temperature, salinity, alkalinity, and DIC values from the nearest surface sampling station were added to the CTD data, which began 5 meters below the surface. The DIC data is interrupted by a missing data point at 120 m. Nitrite (μM) was scaled by a factor of 100 and nitrate (μM) and sulphate (mM) by a factor of 0.1 to fit values on the plot, and are denoted by an asterisk in the legend.

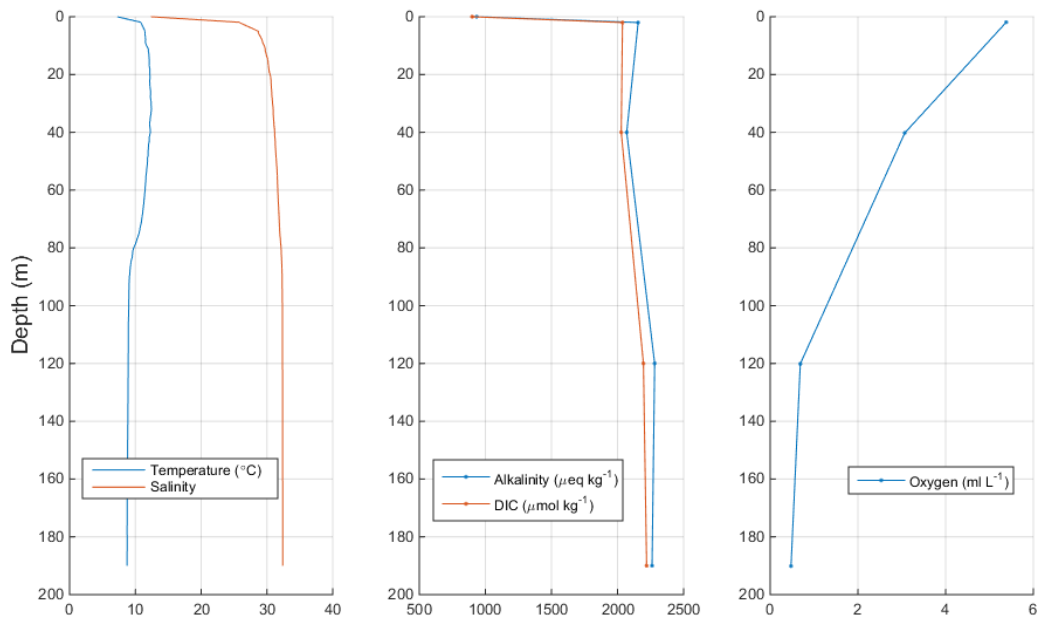


Fig. 9. Temperature, salinity, alkalinity, and DIC from the CTD cast in Tahsis Inlet. Surface (depth of zero) temperature, salinity, alkalinity, and DIC values from the nearest surface sampling station were added to the CTD data, which began 2 meters below the surface.

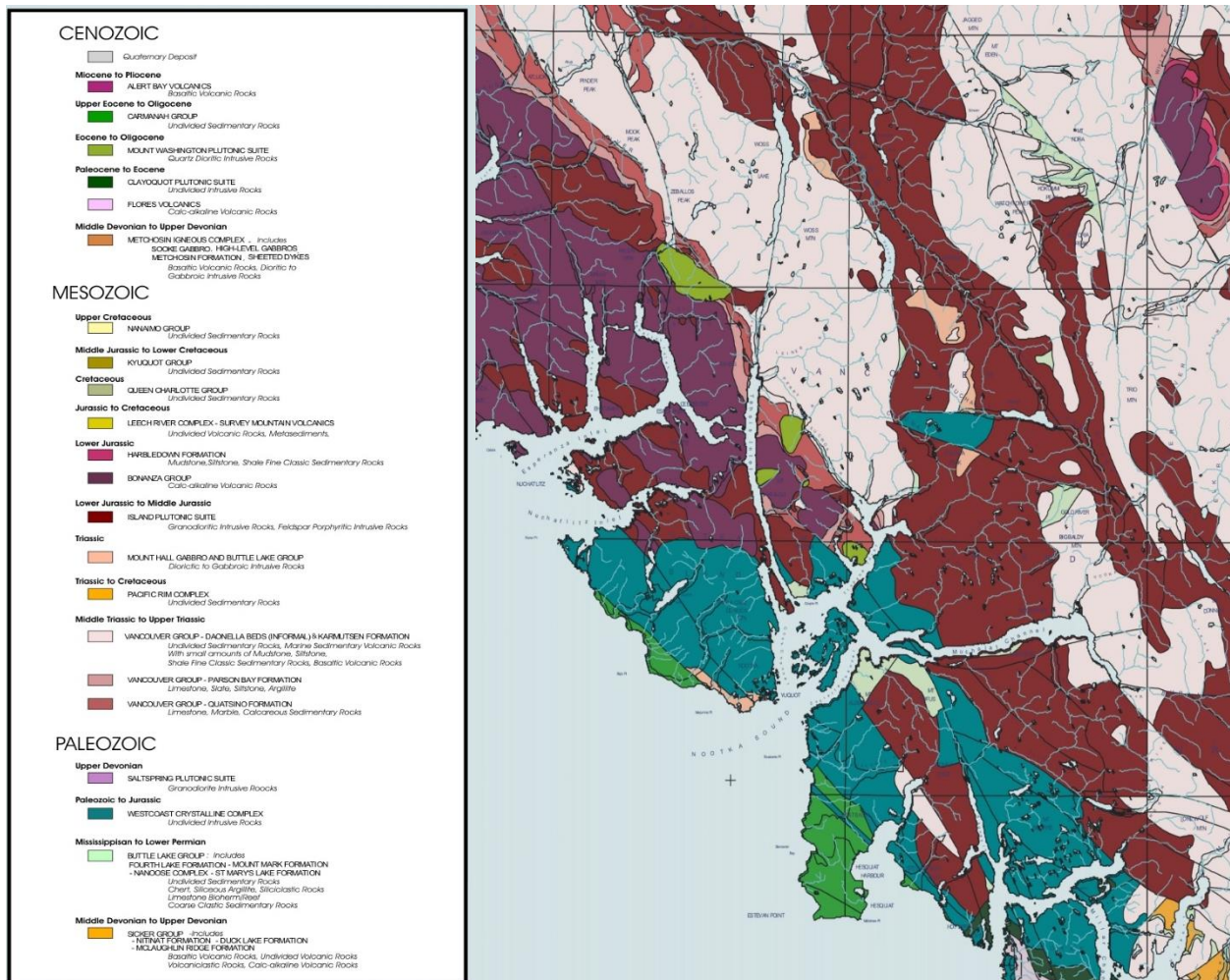


Fig. 10. A map of the bedrock surrounding Nootka Sound. Taken from the publicly accessible Vancouver Island Regional Ecosystems Program site, run by the British Columbia Ministry of Environment. <http://www.env.gov.bc.ca/van-island/pa/programs.html>

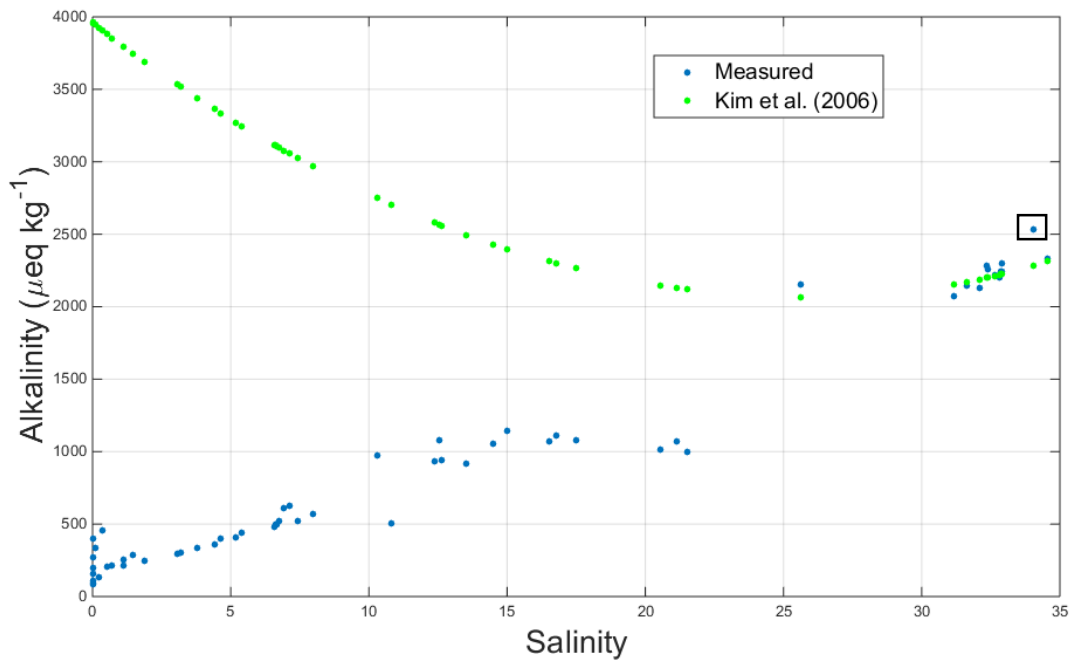


Fig 11. Alkalinity values calculated from temperature and salinity with the algorithm given in Kim et al. (2006), compared against alkalinity values measured in the inlets of Nootka Sound, BC. Values agree within $100 \mu\text{eq kg}^{-1}$ above a salinity of 25 except for the measurement from 500 m depth in the open ocean (boxed).

References

- Abril, G., H. Etcheber, B. Delille, M. Frankignoulle, and A. Borges. 2003. Carbonate dissolution in the turbid and eutrophic Loire estuary. *Mar. Ecol. Prog. Ser.* **259**: 129–138.
- Berner, R. A., and M. R. Scott. 2003. Carbonate alkalinity in the pore waters of anoxic marine sediments. *Limnol. Oceanogr.* **12**: 365–368.
- Brewer, P. G., and J. C. Goldman. 1976. Alkalinity changes generated by phytoplankton growth. **21**: 108–117.
- Cai, W.-J., X. Hu, W.-J. Huang, L.-Q. Jiang, Y. Wang, T.-H. Peng, and X. Zhang. 2010. Alkalinity distribution in the western North Atlantic Ocean margins. *J. Geophys. Res.* **115**: C08014.
- Caldiera, and Wickett. 2003. Anthropogenic carbon and ocean pH. **425**: 234–236.
- Dickson, A. G. 1981. An exact definition of total alkalinity and a procedure for the estimation of alkalinity and total inorganic carbon from titration data. **28**.
- Dickson, A. G., and J. P. Riley. 1978. (Received March 11, 1977; revision accepted August 23, 1977). **6**: 77–85.
- Evans, W., J. T. Mathis, P. Winsor, H. Statscewich, and T. E. Whitley. 2013. A regression modeling approach for studying carbonate system variability in the northern Gulf of Alaska. *J. Geophys. Res. Ocean.* **118**: 476–489.
- Feely, R. a., S. R. Alin, J. Newton, C. L. Sabine, M. Warner, A. Devol, C. Krembs, and C. Maloy. 2010. The combined effects of ocean acidification, mixing, and respiration on pH and carbonate saturation in an urbanized estuary. *Estuar. Coast. Shelf Sci.* **88**: 442–449.
- Feely, R. A., C. L. Sabine, K. Lee, W. Berelson, J. Kleypas, V. J. Fabry, F. J. Millero, S. Science, N. Series, and N. Jul. 2004. Impact of Anthropogenic CO₂ on the CaCO₃ System in the Oceans. **305**: 362–366.
- Friis, K. 2003. The salinity normalization of marine inorganic carbon chemistry data. *Geophys. Res. Lett.* **30**: 1085.
- Goldman, J. C., and P. G. Brewer. 1980. Effect of nitrogen source and growth rate on phytoplankton-mediated changes in alkalinity. *Limnol. Oceanogr.* **25**: 352–357.
- Hieronimus, J., and G. Walin. 2013. Unravelling the land source : an investigation of the processes contributing to the oceanic input of DIC and alkalinity. **1**: 1–10.
- Hiscock, W., and F. J. Millero. 2006. Alkalinity of the anoxic waters in the Western Black Sea. **53**: 1787–1801.
- Hoppema, J. 1990. THE DISTRIBUTION AND SEASONAL VARIATION OF ALKALINITY IN THE SOUTHERN. **26**: 11–23.

- Howland, R. J. ., a. . Tappin, R. . Uncles, D. . Plummer, and N. . Bloomer. 2000. Distributions and seasonal variability of pH and alkalinity in the Tweed Estuary, UK. *Sci. Total Environ.* **251-252**: 125–138.
- IPCC. 2014. *Climate Change 2014: Synthesis Report. Contribution of Working Groups I, II and III to the Fifth Assessment Report of the Intergovernmental Panel on Climate Change.* IPCC, Geneva, Switzerland, 151 pp
- Hydes, D. J., and S. E. Hartman. 2011. Seasonal and inter-annual variability in alkalinity in Liverpool Bay (53.5° N, 3.5° W) and in major river inputs to the North Sea. *Ocean Dyn.* **62**: 321–333.
- Kim, H.-C., and K. Lee. 2009. Significant contribution of dissolved organic matter to seawater alkalinity. *Geophys. Res. Lett.* **36**: L20603.
- Kim, H.-C., K. Lee, and W. Choi. 2006. Contribution of phytoplankton and bacterial cells to the measured alkalinity of seawater. *Limnol. Oceanogr.* **51**: 331–338.
- Knull, J., and F. Richards. 1969. A note on the sources of excess alkalinity in anoxic waters*. **16**: 205–212.
- Lauerwald, R., J. Hartmann, N. Moosdorf, S. Kempe, and P. a. Raymond. 2013. What controls the spatial patterns of the riverine carbonate system? — A case study for North America. *Chem. Geol.* **337-338**: 114–127.
- Lauvset, S. K., N. Gruber, P. Landschützer, a. Olsen, and J. Tjiputra. 2015. Trends and drivers in global surface ocean pH over the past 3 decades. *Biogeosciences* **12**: 1285–1298.
- Lee, K., L. T. Tong, F. J. Millero, C. L. Sabine, A. G. Dickson, C. Goyet, G.-H. Park, R. Wanninkhof, R. a. Feely, and R. M. Key. 2006. Global relationships of total alkalinity with salinity and temperature in surface waters of the world's oceans. *Geophys. Res. Lett.* **33**: L19605.
- Millero, F. J. 2007. The Marine Inorganic Carbon Cycle. 308–341.
- Millero, F. J., K. Lee, and M. Roche. 1998. Distribution of alkalinity in the surface waters of the major oceans. *Mar. Chem.* **60**: 111–130.
- Orr. 2005. *Anthropogenic ocean acidification over the twenty-first century and its impact on calcifying organisms.pdf.*
- Pickard, G. L. 1963. *Oceanographic Characteristics of Inlets of Vancouver Island " British Columbia '.* **0**.
- Spaulding, R. S., M. D. DeGrandpre, J. C. Beck, R. D. Hart, B. Peterson, E. H. De Carlo, P. S. Drupp, and T. R. Hammar. 2014. Autonomous in situ measurements of seawater alkalinity. *Environ. Sci. Technol.* **48**: 9573–81.
- Tjiputra. 2014. Long-term surface pCO₂ trends from observations and models. **1**: 1–24.
- Tully, B. J. P. 1937. *Oceanography of Nootka Sound for publication October.* **3**.

UNESCO. 1983. Technical papers in marine science. **44**.

Voss, B. M., B. Peucker-Ehrenbrink, T. I. Eglinton, G. Fiske, Z. A. Wang, K. a. Hoering, D. B. Montluçon, C. LeCroy, S. Pal, S. Marsh, S. L. Gillies, A. Janmaat, M. Bennett, B. Downey, J. Fanslau, H. Fraser, G. Macklam-Harron, M. Martinec, and B. Wiebe. 2014. Tracing river chemistry in space and time: Dissolved inorganic constituents of the Fraser River, Canada. *Geochim. Cosmochim. Acta* **124**: 283–308.

Wolf-Gladrow, D. a., R. E. Zeebe, C. Klaas, A. Körtzinger, and A. G. Dickson. 2007. Total alkalinity: The explicit conservative expression and its application to biogeochemical processes. *Mar. Chem.* **106**: 287–300.

Zeebe, R. E., and D. a. Wolf-Gladrow. 2001. *CO₂ in Seawater: Equilibrium, Kinetics, Isotopes*, Elsevier.